

Supporting Information

Structural Tuning and Pore modulation of Three Cu(II)-Organic Frameworks: Enhance Stability and Functionality

*Tao Ding, *^a Hao Wang,^a Hui-Min Li,^a Li-Na Zheng, *^a Ning Xue,^a Bo Liu*^b*

a. School of Environmental and Chemical Engineering, Xi'an Polytechnic University, Xi'an 710048, P. R China.

b. College of Chemistry & Pharmacy, Northwest A&F University, Yangling, 712100, P. R. China

Table S1. Selected Bond Length (Å) and Angles (°) for 1 to 3

1			
Cu(1)-O(1)#1	1.981(3)	Cu(2)-O(2)	1.982(3)
Cu(1)-O(1)	1.981(3)	Cu(2)-O(5)	2.22(3)
Cu(1)-O(1)#2	1.981(3)	Cu(2)-O(5A)	2.18(2)
Cu(1)-O(1)#3	1.981(3)	Cu(3)-O(4)	1.949(3)
Cu(1)-O(6)	1.99(2)	Cu(3)-O(4)#4	1.949(3)
Cu(1)-O(6A)	2.223(17)	Cu(3)-O(4)#5	1.949(3)
Cu(2)-O(2)#1	1.982(3)	Cu(3)-O(4)#6	1.949(3)
Cu(2)-O(2)#3	1.982(3)	O(2)#3-Cu(2)-O(2)	88.18(17)
O(1)#2-Cu(1)-O(1)	90.88(18)	O(2)#1-Cu(2)-O(2)	169.63(17)
O(1)#2-Cu(1)-O(1)#3	168.02(17)	O(2)#1-Cu(2)-O(5)	95.9(10)
O(1)#1-Cu(1)-O(1)	168.02(17)	O(2)#3-Cu(2)-O(5)	99.8(9)
O(1)#3-Cu(1)-O(1)	87.87(18)	O(2)#2-Cu(2)-O(5)	90.5(9)
O(1)#1-Cu(1)-O(1)#2	87.87(18)	O(2)-Cu(2)-O(5)	94.4(10)
O(1)#1-Cu(1)-O(1)#3	90.88(18)	O(2)#2-Cu(2)-O(5A)	90.2(7)
O(1)-Cu(1)-O(6)	95.2(8)	O(2)-Cu(2)-O(5A)	98.5(6)
O(1)#3-Cu(1)-O(6)	102.7(9)	O(2)#3-Cu(2)-O(5A)	100.2(7)
O(1)#2-Cu(1)-O(6)	89.3(9)	O(2)#1-Cu(2)-O(5A)	91.8(6)
O(1)#1-Cu(1)-O(6)	96.7(8)	O(4)-Cu(3)-O(4)#5	180
O(1)#1-Cu(1)-O(6A)	95.99(9)	O(4)#6-Cu(3)-O(4)#4	180.00(13)
O(1)-Cu(1)-O(6A)	95.99(9)	O(4)#5-Cu(3)-O(4)#4	88.6(2)
O(2)#1-Cu(2)-O(2)#3	90.88(17)	O(4)-Cu(3)-O(4)#6	88.6(2)
O(2)#1-Cu(2)-O(2)#2	88.18(17)	O(4)#5-Cu(3)-O(4)#6	91.4(2)
O(2)#2-Cu(2)-O(2)#3	169.63(17)	O(4)-Cu(3)-O(4)#4	91.4(2)
O(2)#2-Cu(2)-O(2)	90.88(17)		

Symmetrical codes: #1 -x+1, y, z ; #2 -x+1, y, -z-1/2; #3 x, y, -z-1/2; #4 -x, y, z ; #5 x, -y+1, -z-1; #6-x, -y+1, -z-1 for 1.

2			
Cu(1)-O(2)#1	1.982(5)	Cu(2)-O(3)	1.966(5)
Cu(1)-O(1)	1.970(5)	Cu(2)-O(4)	2.145(8)
Cu(1)-O(6)	1.938(11)	Cu(2)-O(5)#2	1.956(5)
Cu(1)-O(11)	2.135(6)	Cu(2)-O(5)#4	1.956(5)
Cu(1)-O(7)#1	1.977(17)	Cu(3)-O(8)	1.975(4)
Cu(1)-C(9A)#1	2.61(4)	Cu(3)-O(8)#3	1.975(4)
Cu(1)-O(6A)	2.09(3)	Cu(3)-O(9)	2.134(8)
Cu(1)-O(7A)#1	1.94(3)	Cu(3)-O(10)#6	1.973(5)
Cu(1)-O(2)#1	1.982(5)	Cu(3)-O(10)#5	1.973(5)

O(2)#1-Cu(1)-O(11)	97.1(2)	O(7A)#1-Cu(1)-O(11)	88.1(11)
O(2)#1-Cu(1)-O(6A)	88.9(7)	O(3)#3-Cu(2)-O(3)	87.6(3)
O(1)-Cu(1)-O(2)#1	167.8(2)	O(3)-Cu(2)-O(4)	95.6(2)
O(1)-Cu(1)-O(11)	95.2(2)	O(5)#4-Cu(2)-O(3)	91.10(19)
O(1)-Cu(1)-O(7)#1	89.7(5)	O(5)#2-Cu(2)-O(3)	167.9(2)
O(1)-Cu(1)-O(6A)	88.2(7)	O(5)#2-Cu(2)-O(3)#3	91.10(19)
O(6)-Cu(1)-O(2)#1	91.3(4)	O(5)#4-Cu(2)-O(4)	96.5(3)
O(6)-Cu(1)-O(1)	88.6(4)	O(5)#2-Cu(2)-O(5)#4	87.6(3)
O(6)-Cu(1)-O(11)	91.1(10)	O(8)-Cu(3)-O(8)#3	88.5(3)
O(6)-Cu(1)-O(7)#1	168.8(3)	O(8)-Cu(3)-O(9)	95.2(2)
O(7)#1-Cu(1)-O(11)	100.1(9)	O(10)#5-Cu(3)-O(8)	167.8(2)
O(6A)-Cu(1)-O(11)	104.1(11)	O(10)#6-Cu(3)-O(8)#3	167.8(2)
O(6A)-Cu(1)-C(9A)#1	140.6(10)	O(10)#6-Cu(3)-O(9)	97.0(3)
O(7A)#1-Cu(1)-O(1)	91.9(9)	O(10)#6-Cu(3)-O(10)#5	88.9(3)

Symmetrical codes: #1 -x+1, y, z ; #2 -x+1, y, -z-1/2; #3 x, y, -z-1/2; #4 -x, y, z ; #5 x, -y+1, -z-1; #6 -x, -y+1, -z-1 for **2**.

3

Cu(2)-O(1)#1	1.963(4)	Cu(1)-O(4)	1.910(19)
Cu(2)-O(2)	1.970(4)	Cu(1)-O(4A)	1.994(19)
Cu(2)-O(7)	1.964(4)	Cu(1)-O(5A)	1.92(3)
Cu(2)-O(8)#1	1.963(5)	Cu(1)-O(007)	1.95(3)
Cu(2)-N(4)#2	2.123(5)	Cu(1)-N(1)	1.991(5)
Cu(1)-O(9)	2.320(4)	Cu(1)-N(2)#3	1.999(4)
O(1)#1-Cu(2)-O(2)	167.23(19)	O(4A)-Cu(1)-O(9)	99.4(5)
O(1)#1-Cu(2)-O(7)	90.3(2)	O(4A)-Cu(1)-N(2)#3	171.9(5)
O(1)#1-Cu(2)-O(8)#1	86.9(2)	O(5A)-Cu(1)-O(9)	95.5(7)
O(1)#1-Cu(2)-N(4)#2	96.12(18)	O(5A)-Cu(1)-O(4A)	90.7(11)
O(2)-Cu(2)-N(4)#2	96.64(19)	O(5A)-Cu(1)-N(1)	176.9(8)
O(7)-Cu(2)-O(2)	87.9(2)	O(5A)-Cu(1)-N(2)#3	93.3(9)
O(8)#1-Cu(2)-O(2)	92.1(3)	O(007)-Cu(1)-N(1)	171.6(6)
O(8)#1-Cu(2)-O(7)	167.4(2)	N(1)-Cu(1)-O(9)	87.41(15)
O(8)#1-Cu(2)-N(4)#2	96.3(2)	N(1)-Cu(1)-O(4A)	87.7(6)
O(4)-Cu(1)-O(9)	96.7(5)	N(1)-Cu(1)-N(2)#3	87.94(19)
O(4)-Cu(1)-O(007)	84.8(10)	N(2)#3-Cu(1)-O(9)	87.28(15)
O(4)-Cu(1)-N(1)	96.6(6)	Cu(1)-O(9)-Cu(1)#3	95.0(2)

Symmetrical codes: #1 -x+1, y, z ; #1-x+3/2, -y+3/2, -z+1; #2 -x+1, -y+1, -z; #3 x, -y+1, z ; #4-x+1, y, -z ; #5 -x+2, -y+1, -z+1; #6 -x+2, y, -z+1 for **3**.

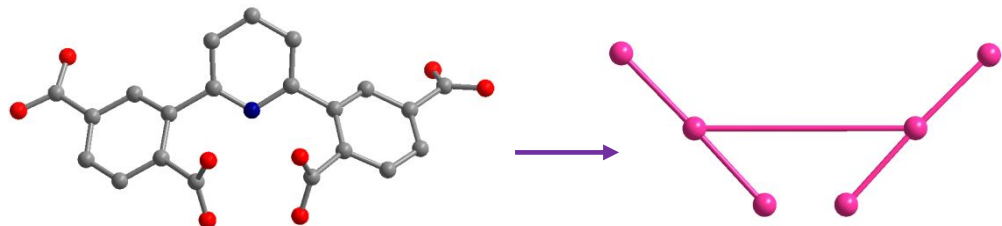


Figure S1. The L^4^- ligand viewed as two 3-c nodes.

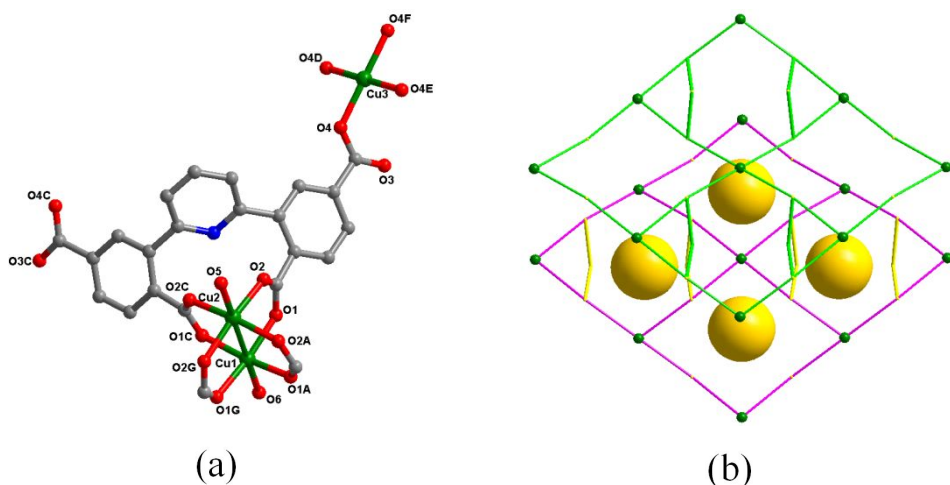


Figure S2. Single-crystal structure of **1**. (a) Coordination environments of Cu(II) ions . The hydrogen atoms are omitted for clarity. Symmetry codes A: $(1-x, y, z)$; B: $(2-x+1, y, -z-1/2)$; C: $(x, y, -z-1/2)$; D: $(-x, y, z)$; E: $(x, -y+1, -z-1)$; F: $(-x, -y+1, -z-1)$; G: $(1-x, y, -z-1/2)$; (gray C, red O, blue N, green Cu); (b) View of the 2D layer structure.

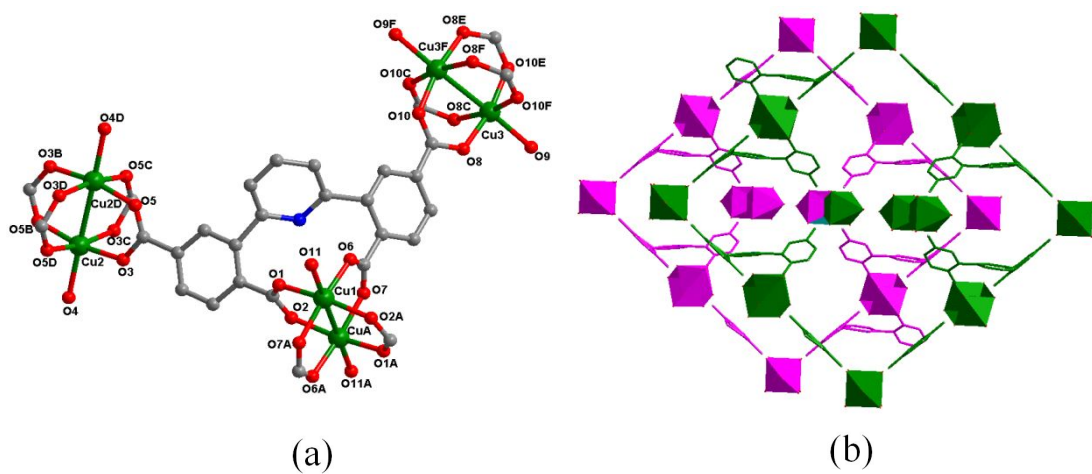


Figure S3. Single-crystal structure of **2**. (a) Coordination environments of Cu(II) ions . The hydrogen atoms are omitted for clarity. Symmetry codes A: $(-x+3/2, -y+3/2, -z+1)$; B: $(-x+1, -y+1, -z)$; C: $(x, -y+1, z)$; D: $(-x+1, y, -z)$; E: $(-x+2, -y+1, -z+1)$; F: $(-x+2, y, -z+1)$; (gray C, red O, blue N, green Cu) ; (b) View of the 2D layer structure

from the c axis.

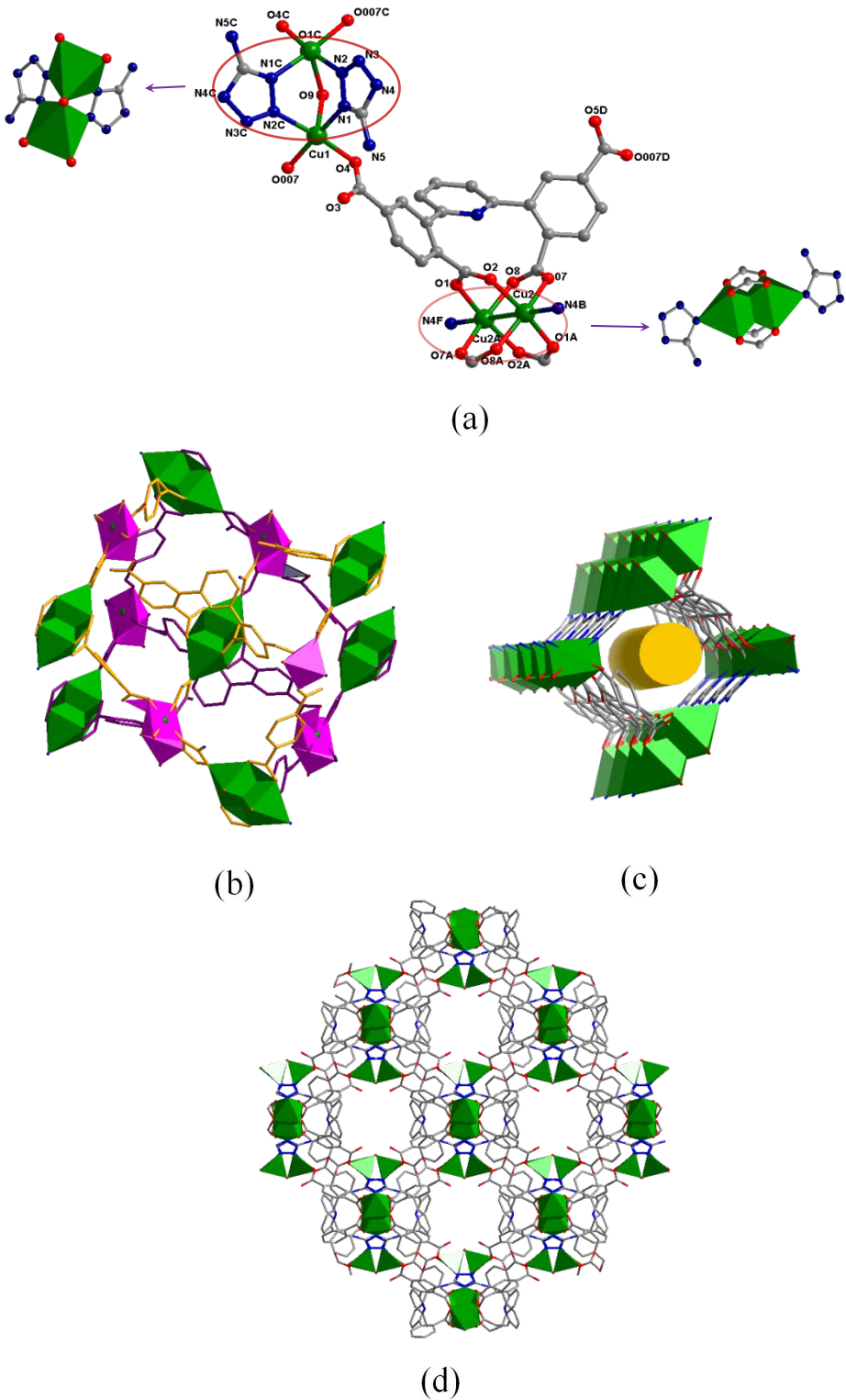


Figure S4. Single-crystal structure of **3**. (a) Coordination environments of Cu(II) ions in **3**. The hydrogen atoms are omitted for clarity. Symmetry codes A: (-x+2, -y+1, -z+1); B: (-x+3/2, -y +3/2, -z+1); C: (-x+1, y, -z+3/2); D: (x, -y+1, z-1/2); E: (x, -y+1,z+1/2); F: (x-1/2, y-1/2, -z+1); (gray C, red O, blue N, green Cu); (b) View of

the 2D layer structure from the b axis; (c) 1D open channel; (d) are stacked diagrams from the c axis.

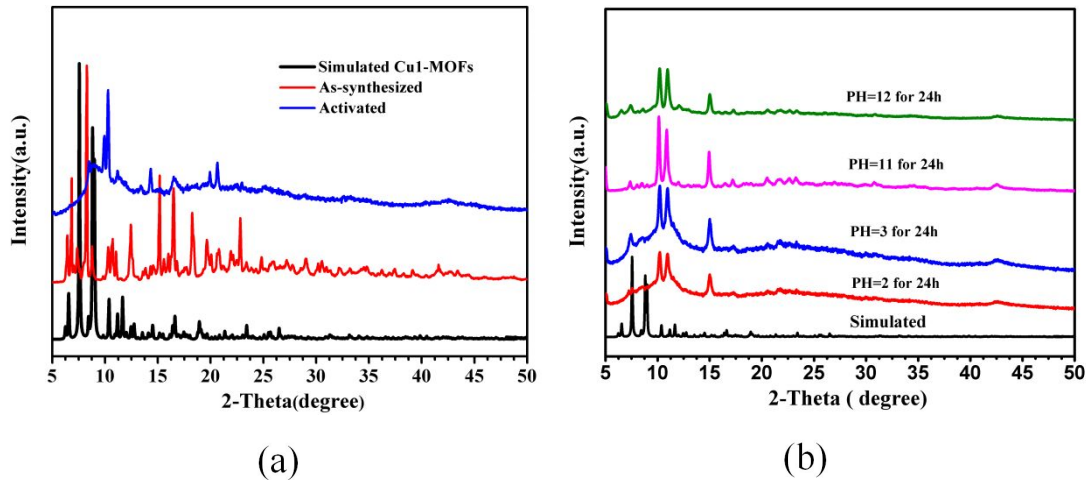


Figure S5. PXRD patterns for **1**. (a) Simulated, as-synthesized and activated samples and (b) After being soaked in acidic and basic solutions for different time periods.

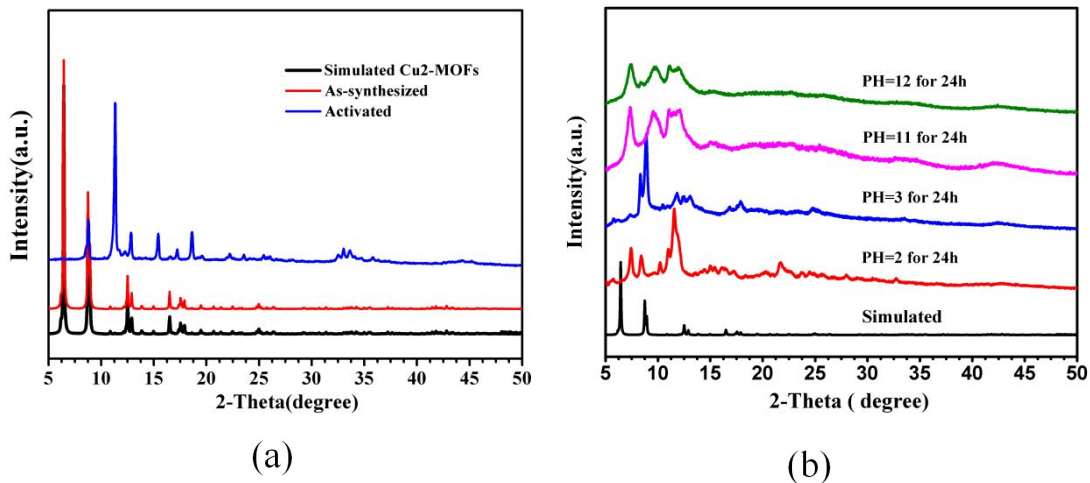


Figure S6. PXRD patterns for **2**. (a) Simulated, as-synthesized and activated samples and (b) After being soaked in acidic and basic solutions for different time periods.

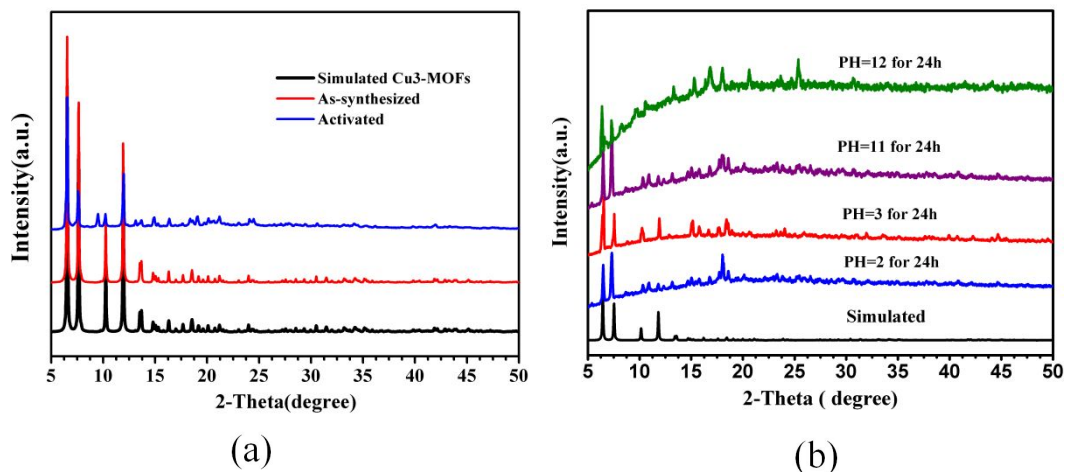


Figure S7. PXRD patterns for **3**. (a) Simulated, as-synthesized and activated samples and (b) After being soaked in acidic and basic solutions for different time periods.

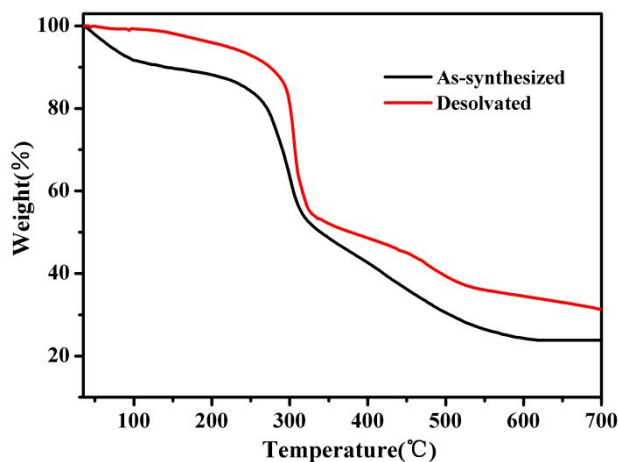


Figure S8. TGA for **1**: as-synthesized and desolved samples.

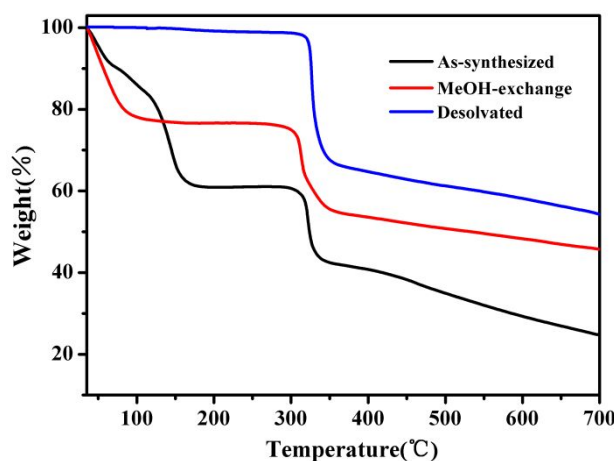


Figure S9. TGA for **2**: as-synthesized, MeOH-exchanged and desolved samples.

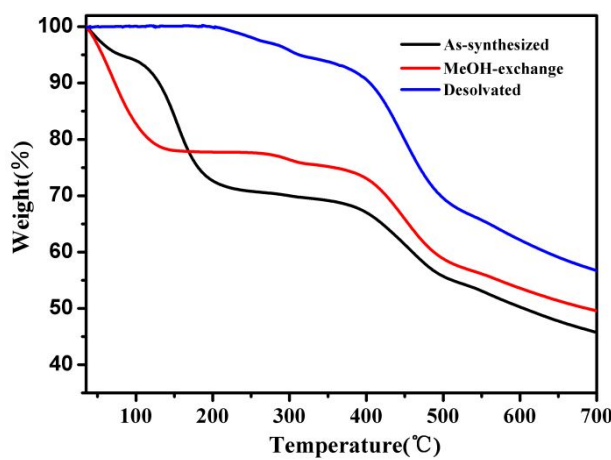


Figure S10. TGA for **3**: as-synthesized, MeOH-exchanged and desolved samples.

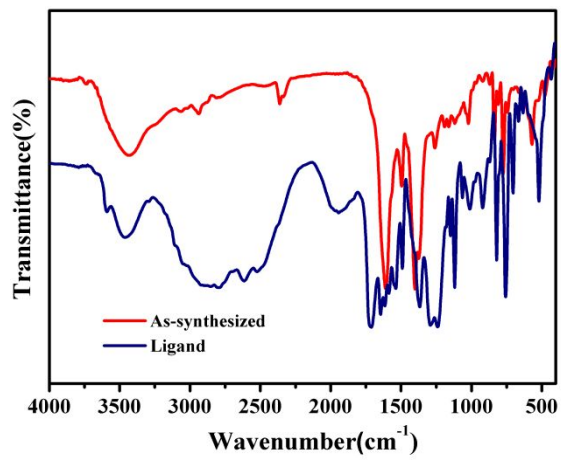


Figure S11. IR for **1**: ligand and as-synthesized samples.

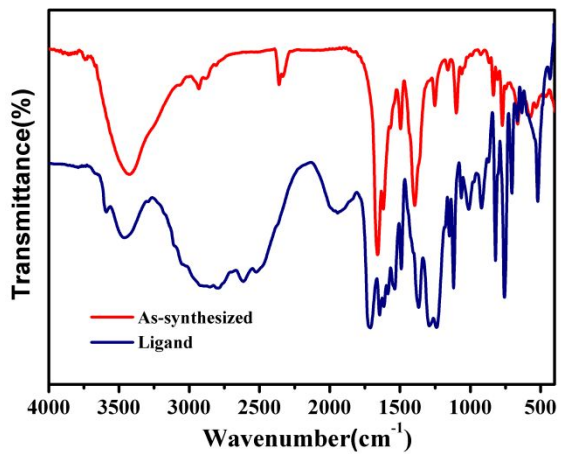


Figure S12. IR for **2**: ligand and as-synthesized samples.

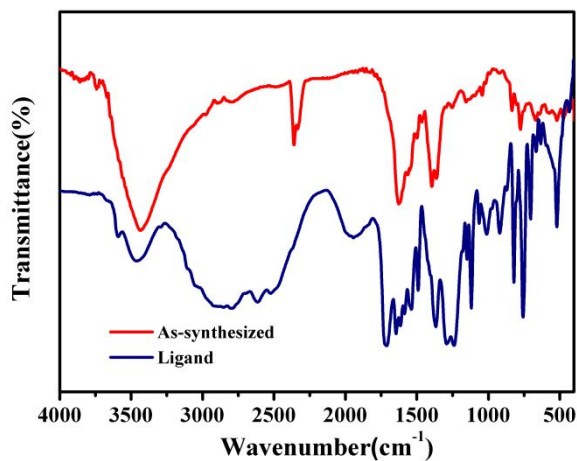


Figure S13. IR for **3**: ligand and as-synthesized samples.

AST adsorption selectivity calculation

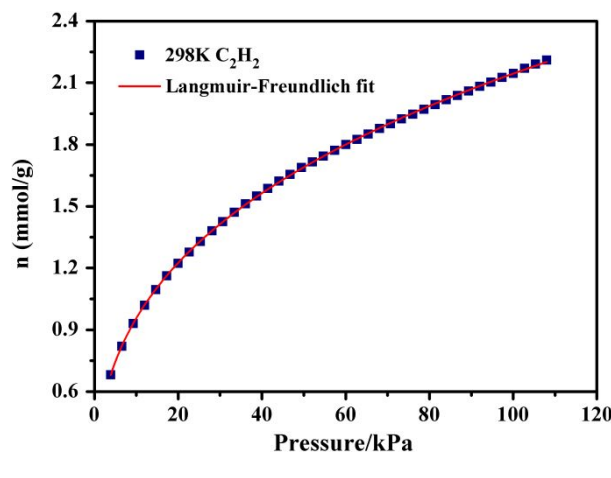
The experimental isotherm data for pure CO₂, CH₄ and N₂ (measured at 298 K) were fitted using a Langmuir-Freundlich (L-F) model

$$q = \frac{a * b * p^c}{1 + b * p^c}$$

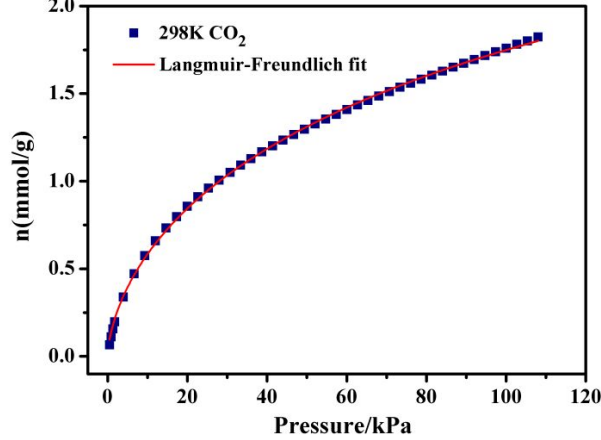
Where q and p are adsorbed amounts and pressures of component i , respectively. The adsorption selectivities for binary mixtures of CO₂/CH₄ at 273 and 298 K and C₂O₂/CH₄ at 298K, defined by

$$S_{ads} = (q_1 / q_2) / (p_1 / p_2)$$

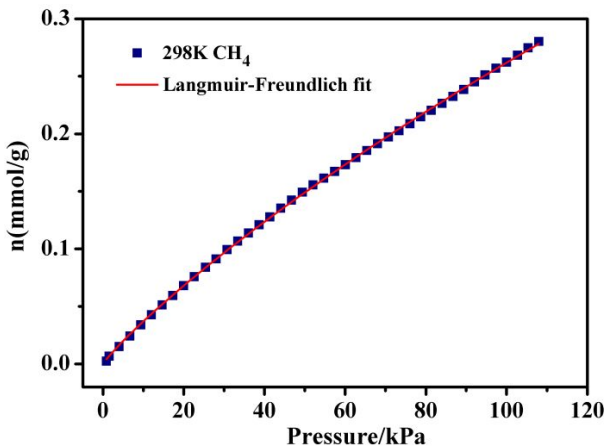
Where qi is the amount of i adsorbed and pi is the partial pressure of i in the mixture.



(a)

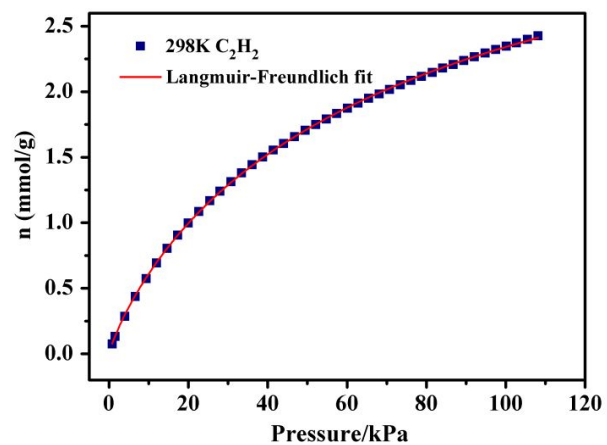


(b)

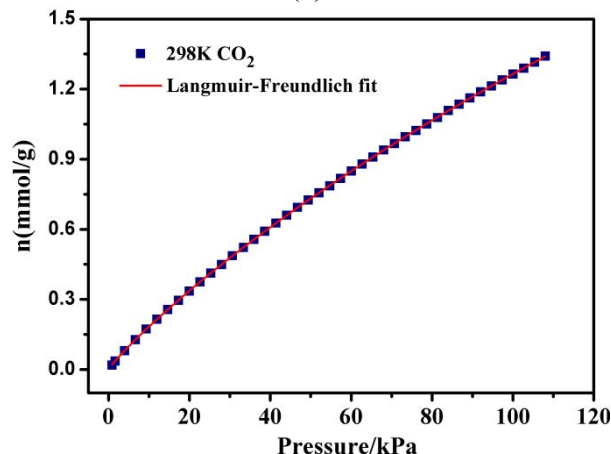


(c)

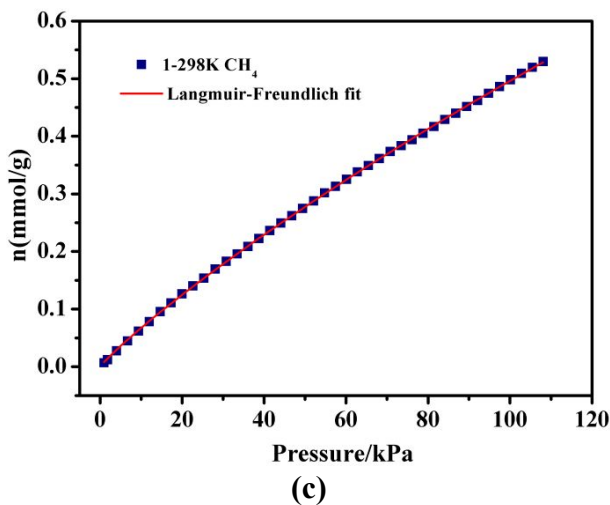
Figure S14. (a) C₂H₂ adsorption isotherms of **1** at 298 K with fitting by L-F model: a =24.31462, b =0.01734, c =0.37322, Chi² = 1.47337E-5, R² = 0.99991; (b) CO₂ adsorption isotherms of **1** at 298 K with fitting by L-F model: a =4.43901, b =0.03524, c =0.633, Chi² =1.59642E-5, R² = 0.99938; (c) CH₄ adsorption isotherms of **1** at 298 K with fitting by L-F model: a = 2.12998, b =0.00224, c =0.89865, Chi² = 1.34179E-6, R² = 0.9998.



(a)

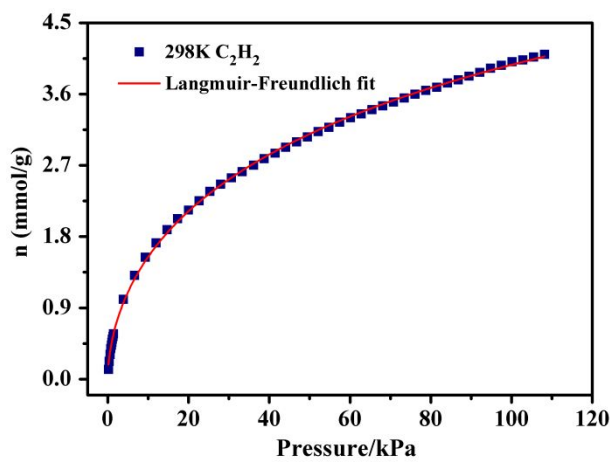


(b)

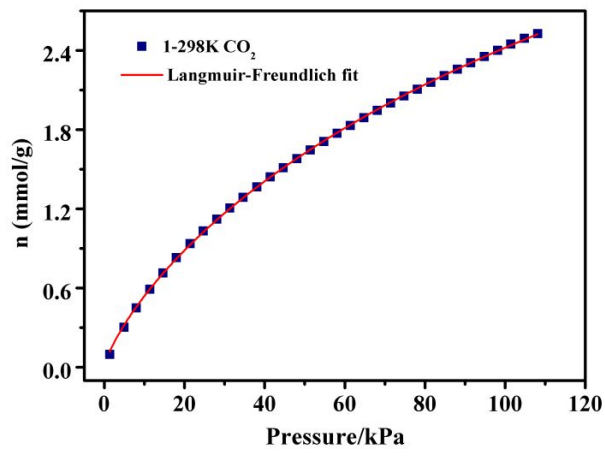


(c)

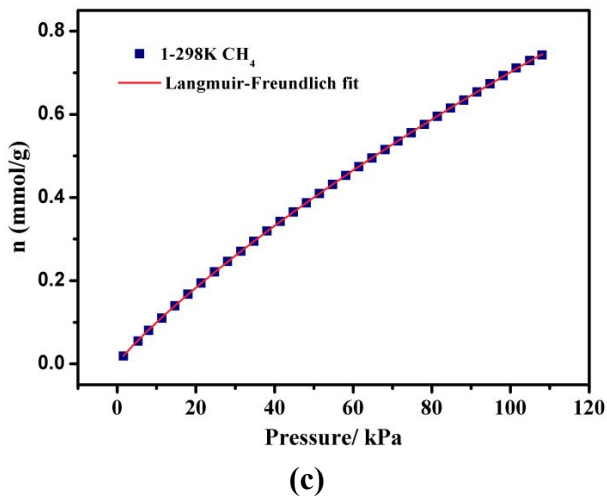
Figure S15. (a) C₂H₂ adsorption isotherms of **2** at 298 K with fitting by L-F model: a = 4.17757, b = 0.02287, c = 0.87318, Chi² = 4.07018E-5, R² = 0.99991; (b) CO₂ adsorption isotherms of **2** at 298 K with fitting by L-F model: a = 7.34815, b = 0.00315, c = 0.9111, Chi² = 9.08482E-7, R² = 0.99999; (c) CH₄ adsorption isotherms of **2** at 298 K with fitting by L-F model: a = 4.86678, b = 0.00173, c = 0.90815, Chi² = 1.7268E-6, R² = 0.99993.



(a)



(b)



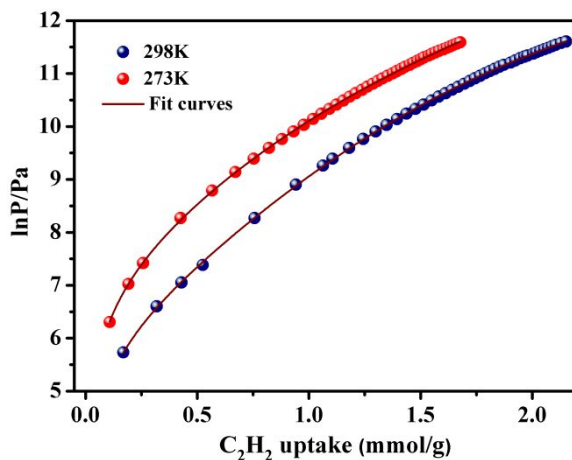
(c)

Figure S16. (a) C₂H₂ adsorption isotherms of **3** at 298 K with fitting by L-F model: a = 9.68477, b = 0.05163, c = 0.56442, Chi² = 7.75771E-4, R² = 0.99952; (b) CO₂ adsorption isotherms of **3** at 298 K with fitting by L-F model: a = 7.51871, b = 0.01254, c = 0.78898, Chi² = 5.44812E-5, R² = 0.99988; (c) CH₄ adsorption isotherms of **3** at 298 K with fitting by L-F model: a = 5.31361, b = 0.0024, c = 0.901, Chi² = 1.18098E-6, R² = 0.99997.

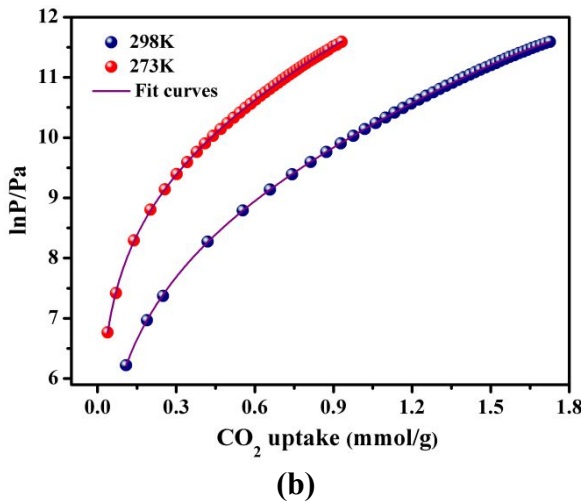
Calculation of sorption heat for C₂H₂ and CO₂ uptakes using Virial 2 model

The above equation was applied to fit the combined C₂H₂ and CO₂ and isotherm data for desolvated **1a** at 273 and 298 K, where P is the pressure, N is the adsorbed amount, T is the temperature, a_i and b_i are virial coefficients, and m and n are the number of coefficients used to describe the isotherms. Q_{st} is the coverage-dependent enthalpy of adsorption and R is the universal gas constant.

$$\ln P = \ln N + 1/T \sum_{i=0}^m a_i N^i + \sum_{i=0}^n b_i N^i Q_{st} = -R \sum_{i=0}^m a_i N^i$$

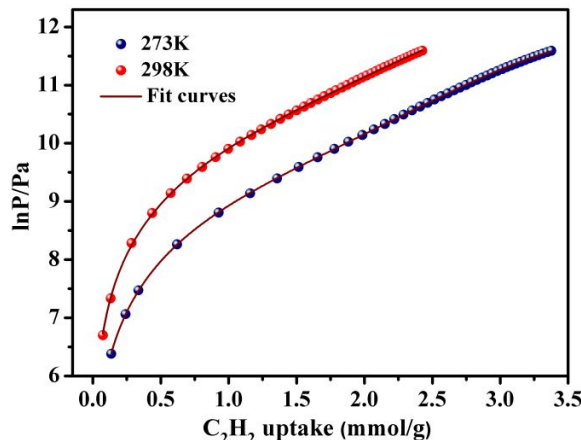


(a)

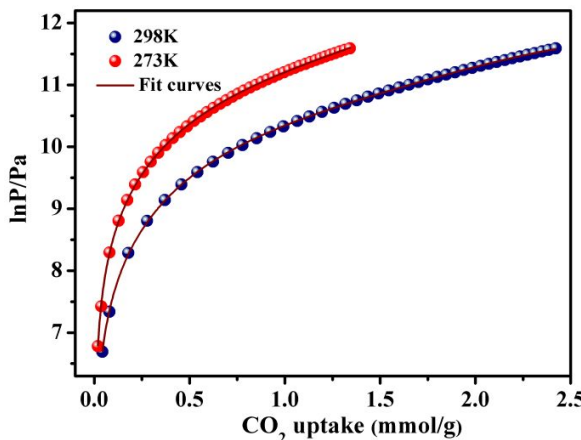


(b)

Figure S17. (a) Virial analysis of the C₂H₂ adsorption data at 298 K and 273 K for **1**. Fitting results: a₀= -3384.23849, a₁ = -2326.22707, a₂ = 3359.65238, a₃ = -1104.86407, a₄ = 45.13798, Chi² = 1.63211E-4, R² = 0.99991; (b) Virial analysis of the CO₂ adsorption data at 298 K and 273 K for **1**. Fitting results: a₀= -5851.66716, a₁ = 1727.35878, a₂ = -2422.53865, a₃ = 1154.05576, a₄ = -78.28237, Chi² = 3.18886E-5, R² = 0.99998.



(a)



(b)

Figure S18. (a) Virial analysis of the C₂H₂ adsorption data at 298 K and 273 K for **2**. Fitting results: a0= -3263.55325, a1 = 282.7658, a2 = -353.66525, a3 =136.96067, a4 = -11.4289, Chi² = 6.25196E-5, R² = 0.99996; (b) Virial analysis of the CO₂ adsorption data at 298 K and 273 K for **2**. Fitting results: a0= -3036.47805, a1 = 559.69175, a2 = -330.64788, a3 =28.47604, a4 = -24.54171, Chi² = 8.01372E-4, R² = 0.99993.

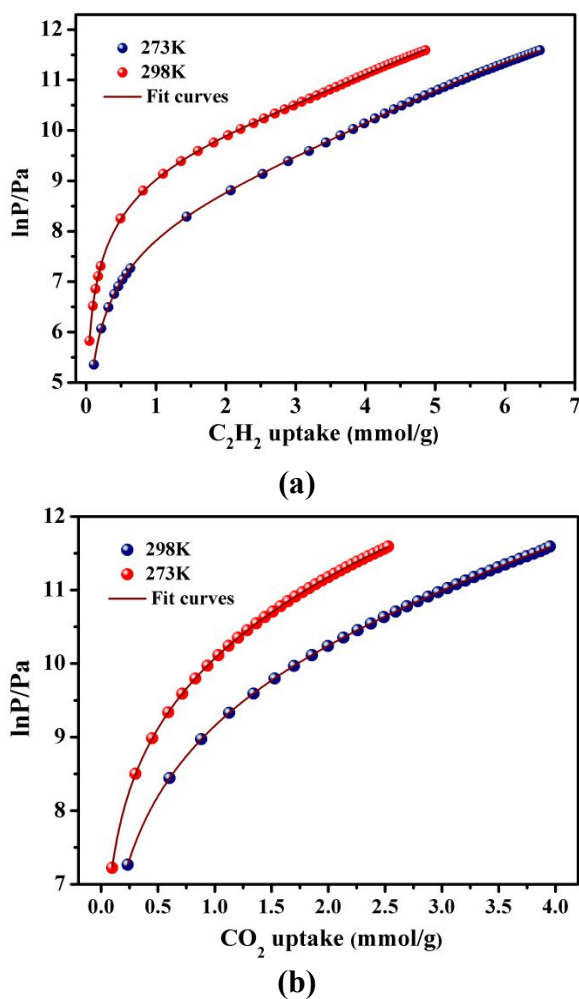


Figure S19. (a) Virial analysis of the C₂H₂ adsorption data at 298 K and 273 K for **3**. Fitting results: a0= -4213.57892, a1 = 296.47929, a2 = -15.7082, a3 =3.9664, a4 = -0.50387, Chi² = 9.48438E-5, R² = 0.99996; (b) Virial analysis of the CO₂ adsorption data at 298 K and 273 K for **3**. Fitting results: a0= -3080.7598, a1 = 264.81468, a2 = -224.48446, a3 =54.16894, a4 = -1.23403, Chi² = 5.7699E-6, R² = 0.99999.